

Pressure-Fluctuation Analysis of a Gas–Solid Fluidized Bed Using the Wigner Distribution

Zhen He

Dept. of Optical and Scientific Instrument Engineering, Zhejiang University, Hangzhou, Zhejiang, 310027, P.R.C.

Dongming Zhang and Bochuan Cheng

UNILAB, Zhejiang University, Hangzhou, Zhejiang, 310027, P.R.C.

Weidong Zhang

Dept. of Optical and Scientific Instrument Engineering, Zhejiang University, Hangzhou, Zhejiang, 310027, P.R.C.

Pressure fluctuations in gas–solid fluidized beds have long been recognized as an important index for the quality of fluidization. Due to their highly random nature, many researchers have resorted to stochastic signal-processing methods to extract useful information. However, methods such as power-spectral density are based on a priori hypothesis of the stationarity of the signals, whose validity has not been investigated. In this article, using the Wigner distribution (WD), the signal's strong nonstationary feature is demonstrated and signal properties are addressed. Local frequency information is extracted from the defined parameter—the local peak weighted average (LPWA), which can be regarded as a generalized concept of the major frequency of power-spectral density in the nonstationary case. Experimental results indicate that LPWA is stochastically much more reproducible than the major frequency of power-spectral density. The change in LPWA under different operating conditions may reflect the corresponding change in the bubble phase. This information is useful in characterizing the quality of fluidization.

Introduction

Fluidized beds are used in a variety of fields including the chemical, metallurgical, food and pharmaceutical industries. Above the minimum bubbling velocity, gas forms bubbles at grid holes. The formation, motion and coalescence of these bubbles are the main causes of pressure fluctuations (Fan et al., 1981). While pressure fluctuations in fluidized beds have been extensively studied by many investigators (Kang et al., 1967; Lirag and Littman, 1971; Lee and Kim, 1988; Carsky et al., 1990; Kage et al., 1991), these phenomena are not fully understood because of their highly random and stochastic nature.

Previous investigators have applied the statistical analysis or correlation approach in analyzing the random pressure-fluctuation signals in the fluidized beds (Shuster and Kisliak, 1952; Bailie et al., 1961; Winter, 1968; Moritomi et al., 1980; Fan et al., 1981; Huang et al., 1986). They have calculated

the probability density, autocorrelation function, and power-spectral density and have gotten a lot of useful information about fluidized beds. Recent works on multiphase flow systems have indicated that the concepts of fractal and multifractal may be applicable to the analysis of fluidized beds (Fan et al., 1990, 1993; Kwon et al., 1994; Bakshi et al., 1995).

Due to the discontinuity of the bubble phase, which is the main contributor to the pressure fluctuation, it is reasonable that the pressure fluctuation signals should bear some characteristics of nonstationarity. Thus, it may be advantageous to resort to time-varying signal-analysis methods, which can reveal local information of pressure-fluctuation signals in fluidized beds. We study the famous Wigner distribution (WD) as a promising candidate to meet this requirement. The WD (also called Wigner–Ville distribution or Wigner–Ville spectrum in the random case) was first introduced in 1932 by Wigner in quantum mechanics and reintroduced in 1948 by Ville for signal analysis. Then in 1980 Claasen and Mecklenbrauker's important set of articles inspired a surge of interest in the study and application of WD. Power-spectral density is

Correspondence concerning this article should be addressed to Z. He.
Permanent address of Z. He: 12-1-402, Youyi Xin Chun, Song Mu Chang, Hangzhou, Zhejiang, 310007, P.R.C.

based on the hypothesis of stationarity, which dooms its global information description of analyzed signals. The advantage of the WD over the power-spectral density is that it can capture the local information of a nonstationary signal, while the latter fails to. WD analysis has been successfully applied to diverse fields from which nonstationary signals arise. Examples include seismic processing (Boashash, 1983), speech (Chester et al., 1984), oceanography (Imberger and Boashash, 1986), and nonlinear systems and chaos (Adamopoulos et al., 1988) to mention only a few. An extensive bibliography can be found in Cohen's excellent review article (Cohen, 1989). In the present article, we apply the WD to pressure-fluctuation analysis in a gas-solid fluidized bed. We first briefly review the definition of the WD and some important properties to help readers understand the rest of the article. Then, we discuss in detail the practical considerations to the specific application. In order to extract useful information from the complicated WD space, a useful and easily implemented parameter referred to as the local peak weighted average (LPWA) is defined. In the experimental section, we outline the experimental facilities and operating procedures, measurements, and computations. In the results and discussion section, we demonstrate the strong nonstationarity of pressure-fluctuation signals and make several important statements relating to the signal's properties. The effectiveness of the LPWA is verified under different operating conditions. We make an effort to interpret the physical results meaningfully by looking at the bubble's behavior. We show its advantage by comparing it with the corresponding result of the major frequency of power-spectral density.

Wigner Distribution: Definition and Properties

In this section we review the definition of the WD and some important properties relevant to its application. Readers with further interest in the WD are referred to Claasen and Mecklenbrauker's articles (1980), where a detailed description of the WD can be found, and a tutorial review written by Cohen (1989).

The cross WD of two signals $f(t)$ and $g(t)$ is defined by

$$W_{f,g}(t, \omega) = \int \exp(-j\omega\tau) f\left(t + \frac{\tau}{2}\right) g^*\left(t - \frac{\tau}{2}\right) d\tau, \quad (1)$$

where the asterisk denotes the complex conjugate. (The integration range in this article is from $-\infty$ to $+\infty$, unless specified otherwise.)

The auto-Wigner distribution of a signal $f(t)$ is then naturally given by

$$W_f(t, \omega) = \int \exp(-j\omega\tau) f\left(t + \frac{\tau}{2}\right) f^*\left(t - \frac{\tau}{2}\right) d\tau. \quad (2)$$

By convention, we call Eq. 2 the WD.

The smoothed Wigner distribution (SWD) is obtained by applying 2-D convolution to the WD in both the time and frequency directions with a function $G(t, \omega)$. We denote SWD as

$$\tilde{W}_f(t, \omega) = \frac{1}{2\pi} \iint W_f(\tau, \xi) G(t - \tau, \omega - \xi) d\tau d\xi. \quad (3)$$

Practically, smoothing in the frequency direction is inevitable because one has to reduce the data to a finite length in order to implement the WD. In many applications, smoothing in both directions is essential to extract explicit and reliable information, though doing so can deteriorate the time-frequency resolution. In other words, one may fail to distinguish the distinct events localized around different time and frequency centers in the WD space due to the blurring effects introduced by excessive smoothing. Thus, some appropriate smoothing that should be orientated by the specific application is very important in capturing the essence of the analyzed signal. We are particularly interested in a class of smoothing where

$$G(t, \omega) = g_1(t)g_2(\omega). \quad (4)$$

Such a kernel allows us to perform independent smoothing in the frequency and time directions, thus providing a very flexible scheme for practical applications.

We now list some important properties of the WD:

Real property:

$$W_f(t, \omega) = W_f^*(t, \omega). \quad (5)$$

Bilinear property:

$$W_{f+g}(t, \omega) = W_f(t, \omega) + W_g(t, \omega) + 2\text{Re}W_{f,g}(t, \omega). \quad (6)$$

The third term in Eq. 6 is the well-known cross term (Flandrin, 1984) that makes it difficult to interpret the WD of multicomponent signals and should be suppressed by some suitable smoothing.

Marginal properties:

$$\frac{1}{2\pi} \int W_f(t, \omega) d\omega = |f(t)|^2 \quad (7)$$

$$\int W_f(t, \omega) dt = |F(\omega)|^2, \quad (8)$$

where $F(\omega)$ in Eq. 8 is the frequency spectrum of $f(t)$.

Time- and frequency-limited properties: If $f(t)$ satisfies

$$f(t) = 0 \quad t < t_a \quad \text{or} \quad t > t_b,$$

then

$$W_f(t, \omega) = 0 \quad t < t_a \quad \text{or} \quad t > t_b \quad \forall \omega. \quad (9)$$

If $f(t)$ satisfies

$$F(\omega) = 0 \quad \omega < \omega_a \quad \text{or} \quad \omega > \omega_b$$

then

$$W_f(t, \omega) = 0 \quad \omega < \omega_a \quad \text{or} \quad \omega > \omega_b \quad \forall t \quad (10)$$

Analytic signal and its WD: $Z(t)$ is called an analytic signal if it is associated with the corresponding real signal $s(t)$ as follows:

$$Z(t) = s(t) + jH[s(t)] \quad \text{where } j = \sqrt{-1} \quad (11)$$

with H representing the Hilbert transform

$$H[s(t)] = \frac{1}{\pi} \int \frac{s(\xi)}{t - \xi} d\xi \quad (12)$$

Then its frequency spectrum vanishes for $\omega < 0$, while the positive part keeps its shape. Consequently, we have

$$W_z(t, \omega) = 0 \quad \omega < 0 \quad \forall t \quad (13)$$

according to Eq. 10. The concept of an analytic signal is important in both implementing the WD practically and in defining the instantaneous frequency (IF).

The IF and WD: Provided $Z(t)$ is an analytic signal denoted by

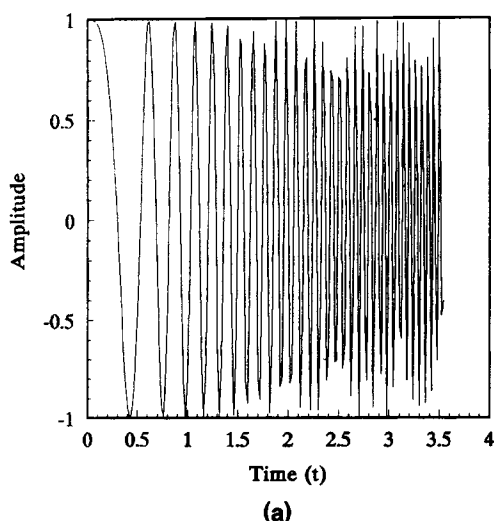
$$Z(t) = a(t) \exp[j\phi(t)]$$

we call the derivative of the phase $\phi(t)$

$$f_i(t) = \frac{d[\phi(t)]}{dt} \quad (14)$$

the instantaneous frequency (IF) of $s(t)$ or $Z(t)$. It is easy to check that the first-order moment of the WD of $Z(t)$ with respect to frequency at time t defined by

$$\Omega_z(t) = \frac{\frac{1}{2\pi} \int \omega W_z(t, \omega) d\omega}{|Z(t)|^2}, \quad (15)$$



supposing $|Z(t)| \neq 0$ and $Z(t)$ is analytic, is equal to the IF of $Z(t)$. We can interpret the result as follows: the physically meaningful frequency components at every occurrence of the WD of a real signal (by using its analytic counterpart to perform the WD) concentrate along the IF. Thus we can regard the IF as the center of the WD at every occurrence. Many scholars (for example, see Boashash, 1992) consider it important to characterize the nature of the time-varying signal, especially for monocomponent signals such as the chirp signal (linear FM). The WD of a chirp signal in contour form is given in Figure 1. (The minimum contour value in this article is about one-quarter the maximum value of the 3-D plot.) Though IF may make more sense in mathematics than in physics, we want the WD concentrates along the IF, which makes the WD faithfully reflect the true frequency distribution at every occurrence.

Since pressure-fluctuation signals in fluidized beds are highly random, we will resort to the WD for the random case. In this situation, $f(t)$ in Eq. 2 will be a random signal. Usually we require $f(t)$ to be an analytic signal. In order to gain a clear explanation of the WD in the random case, we must introduce the concept of the evolutive spectrum (ES) $S(t, \omega)$, which is a natural but not trivial generalization of power-spectral density for nonstationary processes (Priestley, 1965):

$$S(t, \omega) = \int R\left(t + \frac{\tau}{2}, t - \frac{\tau}{2}\right) \exp(-j\omega\tau) d\tau, \quad (16)$$

where

$$R(t_1, t_2) = E[Z(t_1)Z^*(t_2)] \quad (17)$$

is the covariance function of an analytic and harmonizable process $Z(t)$ (a stochastic process is called harmonizable if its covariance function $R(t_1, t_2)$ exists in the bidimensional Fourier transform; an accurate definition can be found in Loeve (1978)), which guarantees the existence of Eq. 16. Substituting Eq. 17 into Eq. 16 and exchanging the integration and expected value, we obtain

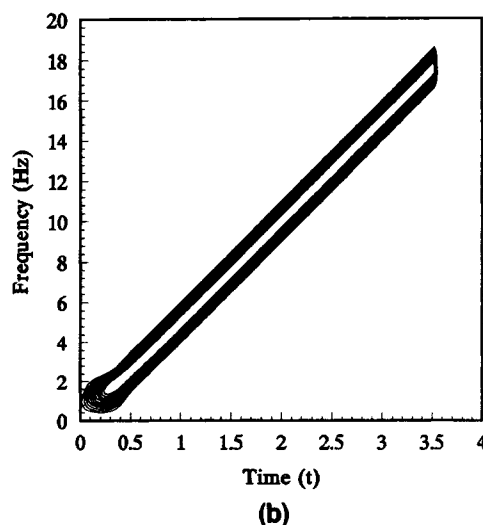


Figure 1. (a) Chirp signal $x(t) = \cos(5\pi t^2)$; (b) contour of WD of the signal.

$$S(t, \omega) = E[W_Z(t, \omega)]. \quad (18)$$

Thus, we find that the WD is an unbiased estimator of the ES that will reduce to power-spectral density if the random process is stationary.

Numerical Implementation and Practical Considerations

In this section, we will focus on the numerical implementation of the WD and some practical considerations of the gas-solid fluidized beds application. The formula we use to calculate the WD is

$$\tilde{W}\left(n, m \frac{\pi}{M}\right) = 2 \sum_{k=-K}^{K-1} \left[\sum_{i=-(I-1)}^{I-1} f(n+k-i) f^*(n-k-i) g(i) \right] h^2(k) \exp\left(-jkm \frac{2\pi}{M}\right) \\ m = 0, 1, \dots, M-1; \quad M = 2K, \quad (19)$$

where $g(i)$ is the frequency window with size $2I-1$ and $h(i)$ is the time window with size $2K$. Actually, Eq. 19 is the discrete version of the SWD defined in Eq. 3. It is the form proposed by Garudadri et al. (1987), whose boundary varies slightly from that in their footnote *i*. Equation 19 implies independent smoothing of the WD in the time and frequency directions, and $f(i)$ is the discrete analytic signal obtained by sampling and performing a Hilbert transform to construct the imaginary part. Since the frequency of the signals in our case is mostly below 15 Hz, we fix the sampling frequency at 50 Hz. Besides those stated in the preceding section, there are two other reasons why we should use the analytic signal instead of its real counterpart. First, since Eq. 19 is periodic with period π , oversampling twice is required to avoid aliasing if the real signal is used directly. Since the negative-frequency component of an analytic signal vanishes, we can use the Nyquist rate without aliasing (Claasen and Mecklenbrauker, 1980). Furthermore, the crossterm created by the interference between the positive and negative frequency can be canceled simultaneously, which may greatly improve the interpretability of the WD.

In order to successfully apply the WD to the pressure-fluctuation signal analysis, several other important factors should be taken into account. They are reduction in estimated variance reduction, sensitivity to nonstationarity, insensitivity to noise, enough frequency resolution in the WD, cross-term suppression. Unfortunately, some of the requirements contradict themselves. The longer the frequency window $g(i)$, which means longer smoothing in the time direction, the better the suppression of noise (Stankovic and Stankovic, 1993), and for the crossterm in the time direction, the more the estimated variance decreases, but at the price of less sensitivity to the nonstationarity (Martin and Flandrin, 1986). Thus, a compromise has to be made in choosing the frequency window $g(i)$. In order to obtain sufficient estimated variance reduction with limited frequency window length, we choose a rectangular window like $g(i)$. With this choice, estimated variance is inversely proportional to the window length (Martin and Flandrin, 1983). Martin and Fl-

drin (1986) suggested that one should perform the smoothing in the time direction within the local stationary time segment in order to keep maximum nonstationary characteristics. Unfortunately, because of the capricious nature of the pressure-fluctuation signals, it is hard to theoretically describe the most appropriate length of the frequency window. In our case, after extensive simulations and comparisons, we recommend a length of 15 (0.3 s) as a satisfactory compromise. In fact, the smoothness and apparent presentation of nonstationarity in the contours of the WDs in Figures 5 and 7 indicates the good bargain we have made.

We also introduce the Gaussian window defined by Harris (1978)

$$h(i) = \exp\left[-\frac{1}{2}\left(a \frac{i}{N/2}\right)^2\right] \\ i = -\frac{N}{2}, -\frac{N}{2} + 1, \dots, 0, \dots, \frac{N}{2} - 1 \quad (20)$$

as the time window. The Gaussian window is an extremely concentrated window, and has a very low side lobe whose time-bandwidth product achieves the equality of the uncertainty principle. The selected time window parameters are as contradictory as those for the frequency window: the larger they are, the better the frequency resolution, but the worse the cross-term suppression in the frequency direction. In our case, the parameters $N = 64$ and $a = 3.0$, yield the optimal tradeoff.

We provide a simulation to demonstrate the logic of the parameter selection. In order to well reflect and easily simulate the features of the practical signal, we choose the three-Gaussian signal as a model:

$$g(t) = \sum_{i=1}^3 \exp\left[-8(t-t_i)^2\right] \cos(2\pi f_i t) \\ t_1 = 1.2, \quad t_2 = 2, \quad t_3 = 3; \\ f_1 = 4, \quad f_2 = 3, \quad f_3 = 4.5 \quad (21)$$

The constants were chosen to match the likely range of frequencies encountered in a typical pressure-fluctuation signal and its time-varying feature. The result is shown in Figure 2, where we can clearly distinguish three Gaussian signals emerging from different time and frequency centers.

Definition of Local Peak Weighted Average and its Estimation

In this section, we will define a useful parameter for extracting local information about the pressure fluctuation signals in fluidized beds from the WD.

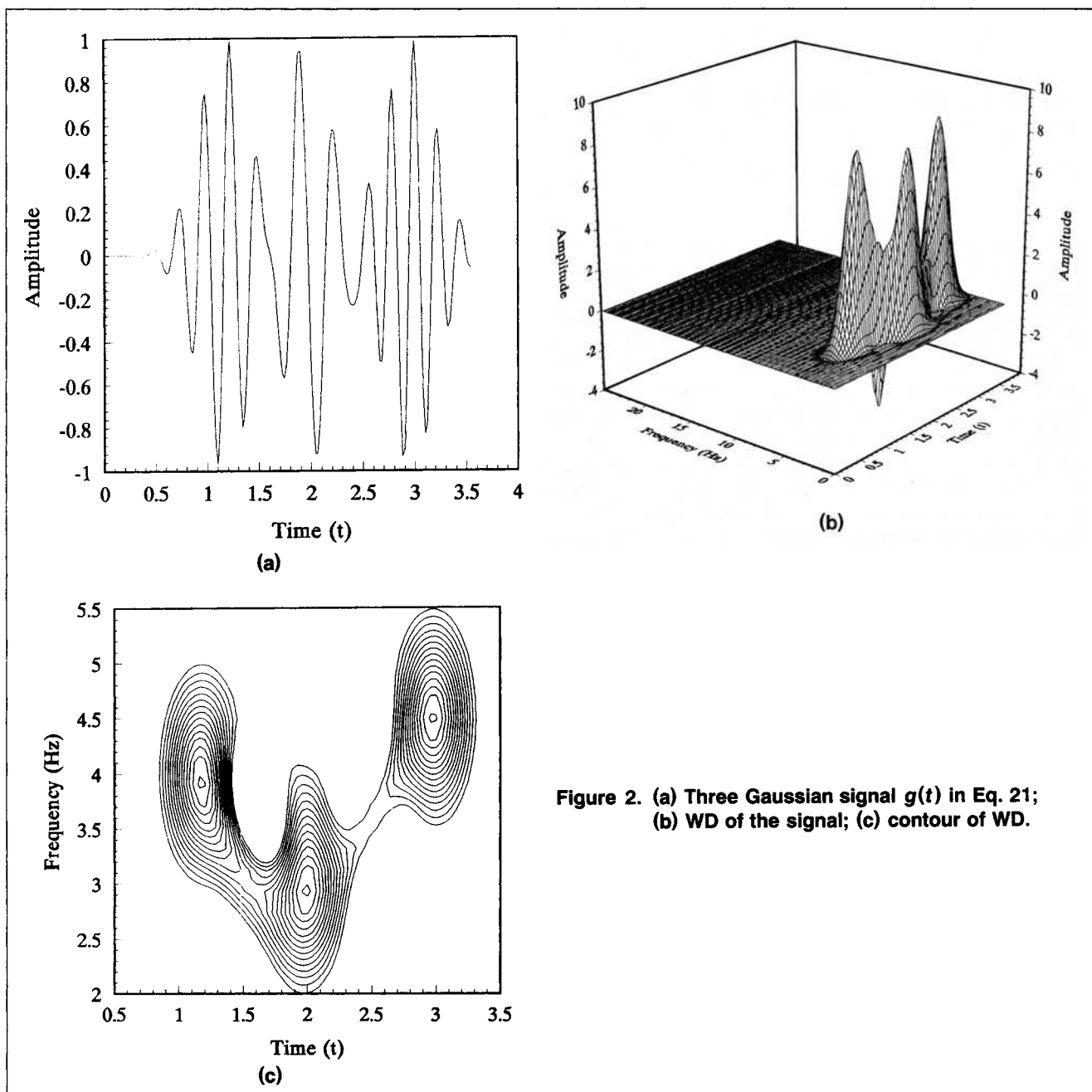


Figure 2. (a) Three Gaussian signal $g(t)$ in Eq. 21; (b) WD of the signal; (c) contour of WD.

Although several natural parameters of the WD exist, such as the IF group delay (GD) (Boashash, 1992), it is difficult to adapt them to this application because of the signals' complicated structure. Because of the influences from diverse phenomena, such as bubbling, the motion of the particle, and the jetting in the fluidized beds, the pressure-fluctuation signals are highly random and complicated multicomponent signals that were also verified by the WD in our experiments. This situation prevents us from interpreting these parameters in a physically meaningful way. Thus we need to explore a new parameter that is specially suitable for characterizing the WD of pressure-fluctuation signals in fluidized beds.

Mainly because of the time-varying nature of the bubble behavior, the frequency content changes notably at different times (refer to Figures 5 and 7). But, as our experiments indi-

cated, it is generally impossible to have more than one comparable apparent frequency peak at every occurrence. This result can be explained by the fact that only one class of bubbles or one bubble contributes most to the local pressure fluctuation near the probe each time. Thus the value of the maximum frequency peak at every occurrence may well reflect the local time bubble behavior in the measuring field. We will call it the local dominant frequency (LDF), denoted as $f_d(t)$. Consequently, we denote the amplitude of LDF as $A_d(t)$. In fact, $f_d(t)$ is exactly the IF if the signal is monocomponent. We have the following expressions:

$$A_d(t) = \sup_{\omega \in [0, +\infty)} S(t, \omega) = \sup_{\omega \in [0, +\infty)} E[W_Z(t, \omega)] \quad (22)$$

$$f_d(t) = \frac{\omega_d(t)}{2\pi}, \quad (23)$$

where sup represents supremum, $S(t, \omega)$ is the ES, and $\omega_d(t)$ satisfies

$$A_d(t) = S(t, \omega_d(t)). \quad (24)$$

In practice, since the power-spectral density is bounded by the frequency-limited property, Eq. 10, $f_d(t)$ is attainable. We can therefore replace sup in Eq. 22 with max.

Since the pressure-fluctuation signal is highly random, the signal's implicit statistical properties hidden in the WD space—those related to the statistical features of the bubbles that are the main cause of the hydrodynamic activity in a fluidized bed—are interesting to use. Thus one has to use statistical methods to find the values in the WD space. In other words, though the values expressed in the WD space at every fixed time t may well link with the local bubble's properties at that time, one should consider such local time-frequency information jointly to obtain the desired statistical information about bubbles, because of the inherently random nature of the bubble phase. Based on $A_d(t)$ and $f_d(t)$, we define a parameter called the local peak weighted average (LPWA) denoted as \bar{f}_d :

$$\bar{f}_d = \lim_{T \rightarrow +\infty} \frac{\int_0^T f_d(t) A_d(t) dt}{\int_0^T A_d(t) dt}, \quad (25)$$

where we assume the signal is zero when $t < 0$. The amplitude weight is used in order to take the intensity of the LDF into account. Normalization is performed in the denominator. Since both $f_d(t)$ and $A_d(t)$ fluctuate between certain values and within certain boundaries, respectively, we can expect \bar{f}_d to be stable for a large data set. This limitation will be ignored for all practical purposes, since the data always have finite length. In our exhaustive experiments, $\bar{f}_d(t)$ is rather stable with large T , for which we will give the experimental results later. If the random process is stationary, $S(t, \omega)$ is independent of time t , as are $A_d(t)$ and $\bar{f}_d(t)$. In that case, $\bar{f}_d(t)$ is clearly the major frequency of the power-spectral density. Thus we can regard $\bar{f}_d(t)$ as a natural generalization of the concept of major frequency in the nonstationary case. LPWA is useful because it shows more explicitly and accurately the influence of the local time bubble behavior in the measuring field, which is the main cause of the local pressure fluctuation. Since different LDF and the corresponding amplitude exist at a different time, the major frequency cannot well reflect the main local information. In fact, we can consider that it is the result of the competition of the different LDFs at different times (refer to the marginal property, Eq. 8). In this sense, we can regard the major frequency in the power-spectral density as an impure version of the LWPA in the nonstationary case.

In the discrete case, assuming that the signal is obtained by the sampling period T , the estimation of Eq. 25 is given by

$$\bar{f}_d = \frac{\sum_{i=0}^{N-1} A_d(i) f_d(i)}{\sum_{i=0}^{N-1} A_d(i)}, \quad (26)$$

where

$$A_d(i) = \max_m W_z\left(i, m \frac{\pi}{M}\right) = W_z\left[i, m_0(i) \frac{\pi}{M}\right] \quad (27)$$

and

$$f_d(i) = \frac{m_0(i)}{2MT}, \quad (28)$$

where

$$m = 0, 1, \dots, M-1 \quad m_0(i) \in \{0, 1, \dots, M-1\} \\ i = 0, 1, \dots, N-1.$$

As stated before, if we maintain enough frequency resolution in the frequency direction and apply sufficient smoothing in the time direction, which can consequently reduce the estimation variance, we can obtain a satisfactory estimation of the LPWA with large N . In our experiments, with the sampling period $T = 0.02$ s, we used 2,048 samples to arrive at an estimate. In order to increase the calculated frequency point density at a fixed time, we doubled the length of the time window by complementing zeros. By calculating the WD every two samples in the time direction, which means $N \approx 1,000$ (practically, we did not calculate the WD of some initial and last samples due to the finite data-length effect), we obtained a rather stable estimation. One should be able to achieve greater stability by using a less restrictive data length.

Experimental Studies

The facilities and procedure employed in carrying out our experiments and measurements are described in this section.

Facilities

A diagram of the experimental facilities is shown in Figure 3. The fluidized-bed assembly includes a bed column, a distributor, and a plenum chamber. The bed is 0.114 m in diam-

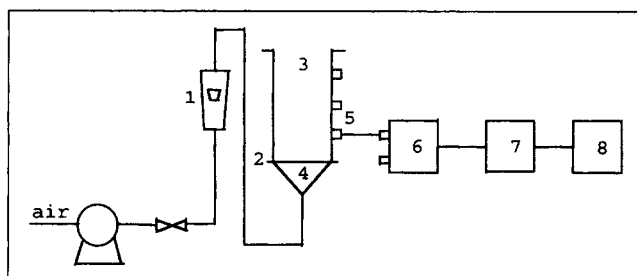


Figure 3. Experimental setup.

(1) Rotameter; (2) distributor; (3) bed; (4) plenum; (5) pressure probes; (6) pressure transducers; (7) A/D board; (8) computer.

Table 1. Solids Characteristics

PE Particles	
Particle density, kg/m ³	962
Apparent density, kg/m ³	454
Average particle size, μm	470
Minimum fluidization velocity, m/s	0.101

eter and 2 m high. The characteristics of the polyethylene (PE) particles can be found in Table 1. The fluidizing fluid is air. The holes on the distributor are 1.5 mm in diameter and have a fractional open area of 1%. Pressure probes are installed on the wall of the bed column at three different heights: 0.05 m, 0.10 m, 0.20 m. For convenience, we index the probes 1, 2, 3, respectively. The outside opening of each pressure probe is connected to one of the two input channels of a differential pressure transducer, which produces an output voltage proportional to the pressure difference between the two channels. The remaining channel is exposed to the atmosphere. The working capacity of the transducer is ± 5 kPa, and the relative accuracy error is $\pm 0.5\%$. The sensitivity of the measuring system is 1 V/kPa.

Procedure

The range of experimental conditions is listed in Table 2. For each run of the experiment, the pressure-fluctuation signals are detected by connecting the pressure probe to the pressure transducer, and subsequently transferring them to the main computer through an analog/digital (A/D) board. The sampling frequency and data length were described in the previous section. After obtaining the data set, we calculated its power-spectral density (we used a variation of the averaged periodogram method proposed by Welch (1967)). Since, in our case, almost all interesting frequency directly related to the behavior of bubbles (especially larger bubbles), which are the main contributor to the pressure fluctuations, concentrate below 15 Hz, we filtered out the frequency above 15 Hz in order to better reflect the influence of the bubbles

Table 2. Experimental Operating Conditions

Experimental Variables	Test Range
Superficial gas velocity, m/s	0.109–0.272
Ratio of static bed height to bed diameter, H_s/D_t	1.4–2.2
Distance above distributor, m	0.05–0.20

in the WD space. The frequency below 0.2 Hz, which can be regarded as low-frequency noise, is also filtered out before calculating the WD. Then we calculated the WD with the parameters described earlier. Consequently, we got the LDF and its amplitude. Finally, we determined the LPWA by Eq. 26. We repeated the experiments ten times for every fixed operating condition and averaged the results of the LPWAs.

Results and Discussion

Figure 4 shows a segment of a typical pressure-fluctuation signal and the power-spectral density of the signal. The results of the WD analysis are presented in Figure 5. The WD in 3-D form is plotted in Figure 5a. In order to get a clear picture of the structure of the WD, we plotted its contour in Figure 5b. Furthermore, we drew the corresponding LDF and its amplitude charts in Figure 5c and 5d. Figures 6 and 7 are the results of another typical signal. As expected, the signals' nonstationarity is shown in Figures 5 and 7. The WD takes a very different shape and amplitude at different times. The amplitude of the whole frequency range in some time interval is so small that a gap eventually emerges (e.g., the time intervals 0 ~ 0.5 s, 2 ~ 2.5 s in Figure 5b). This result is surprising. Neogi et al. (1988) considered that any of the pressure-fluctuation signals from a gas-solid fluidized bed consisted of two components, a periodic component and a random component. Assuming that the signal is ergodic and stationary, they derived the power-spectral density and its single maximum from a model. If their model is consistent with reality, one should expect no such obvious fluctuation of the frequency content at different times. In other words, the WD

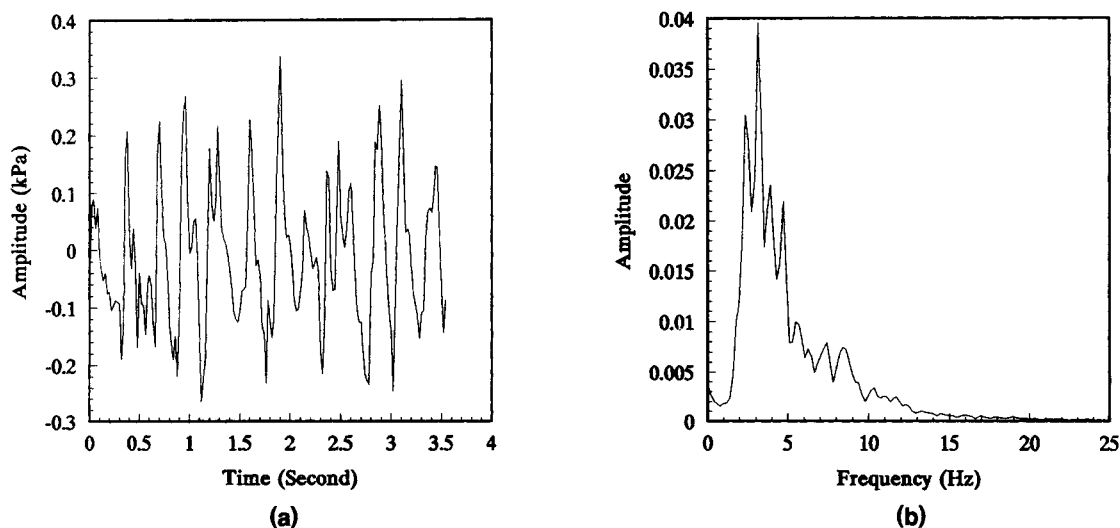


Figure 4. (a) Segment of a typical pressure fluctuation signal with $u = 0.218$ m/s, $D_t = 114$ mm, $H_s/D_t = 1.8$, probe 1; (b) power spectral density of the signal.

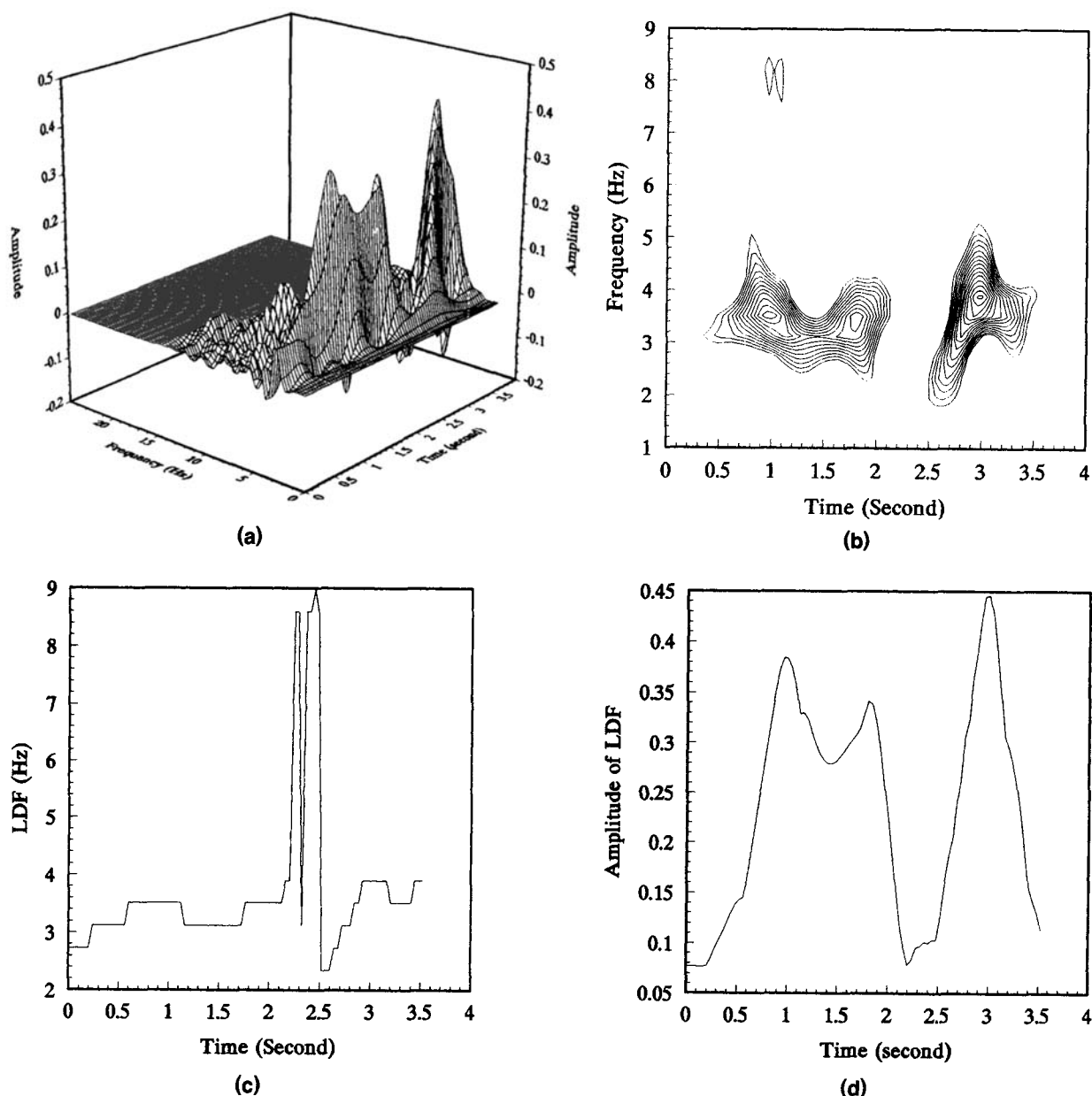


Figure 5. (a) WD of the signal in Figure 4(a); (b) contour of WD; (c) LDF of WD; (d) amplitude of LDF.

should concentrate along the single maximum of the power-spectral density with comparable amplitude every time since the WD will degrade to power-spectral density in the stationary case, which means its frequency content is irrelevant to time t . Thus our results don't support the model. Furthermore, the form of the WD infers that the pressure-fluctuation signals may consist of successive impulses located around different time and frequency centers (see especially Figures 5b, 5d, 7b and 7d), which we think conforms with the discontinuity of the bubble phase. Also, we discovered that, though the location changed, no more than one comparable frequency peak could be detected each time. We explained this fact in the previous section when we defined the LPWA. Though there exists only one major frequency in Figures 4b and 6b, if one studies the plots, one can see that several mi-

nor but obvious peaks occur near the major frequency. This phenomenon can also be seen in Neogi's article (1988; refer to his Figures 12–17). But in the Neogi model only one peak exists in the power-spectral density. The structure of the WD shows why. From Eq. 8, we know that integration of the WD over time leads to the power-spectral density. Since the LDF changes over time, the integration operation causes competition among different LDFs. As a result, the winner becomes the major frequency, while some others became the minor peaks in the power-spectral density.

The LPWA (\bar{f}_d) vs. superficial gas velocity and the probe distance above the distributor, respectively, are shown in Figure 8. Taking the distance above the distributor, h , as a parameter, a steep increase in \bar{f}_d appears in low superficial gas velocity range. After a certain superficial gas velocity, \bar{f}_d de-

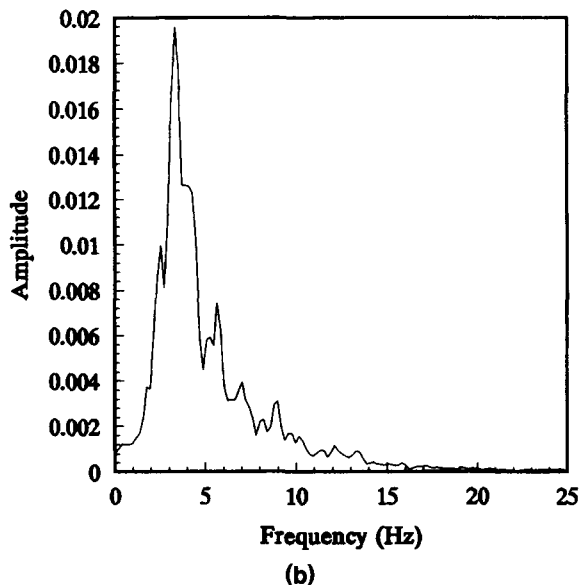
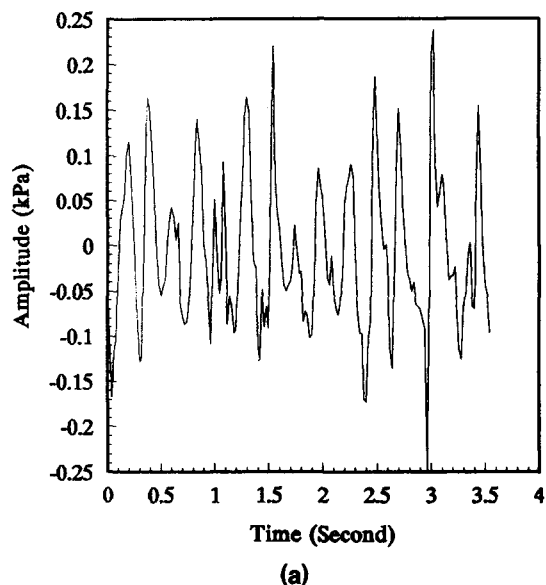


Figure 6. (a) Segment of a typical pressure fluctuation signal with $u = 0.272$ m/s, $D_t = 114$ mm, $H_s/D_t = 1.8$, probe 2; (b) power spectral density of the signal.

creases with an increase in superficial gas velocity. We can attribute this to the fact that the effects of superficial gas velocity on bubble frequency differ in different ranges, which results in the change in \bar{f}_d . When the superficial gas velocity is barely higher than minimum fluidization, an increase in superficial gas velocity mainly causes an increase in the number of bubbles in the fluidized bed, thus increasing the bubble frequency and the \bar{f}_d of the pressure fluctuation. After a certain superficial gas velocity when bubbling is sufficient, the increase in the superficial gas velocity primarily causes an increase in bubble size. From the Darton model (Darton et al., 1977), it is known that the bubble diameter

$$D_b \sim (u - u_{mf})^{2/5} h^{4/5} \quad (29)$$

at a height h and a superficial gas velocity u in the bed. Therefore the bubble volume

$$V_b \sim D_b^3 \sim (u - u_{mf})^{6/5} h^{12/5}. \quad (30)$$

Since the bubble frequency

$$f_b = A_t(u - u_{mf})/V_b, \quad (31)$$

where A_t is the cross-sectional area of the bed. Substituting Eq. 30 into Eq. 31, we get

$$f_b \sim (u - u_{mf})^{-1/5} h^{-12/5}. \quad (32)$$

It is clear now that f_b decreases as either the height h or the superficial gas velocity u increases. Since each bubble is a

source of hydrodynamic activity, this can explain the trends in Figure 8: \bar{f}_d tends to decrease with an increase in the superficial gas velocity u after a certain value; \bar{f}_d tends to decrease with an increase in probe distance above the distributor at a fixed superficial gas velocity.

The ratio of static bed height to bed diameter has a pronounced effect on \bar{f}_d , as shown in Figure 9. Apparently \bar{f}_d decreases as the static bed height increases. Verloop and Heertjes (1974) derived an expression from the particle motion that gives the major frequency to the static bed height as

$$f_m \sim H_s^{-1/2}. \quad (33)$$

Since \bar{f}_d can be regarded as a generalization of f_m in the nonstationary case and has a meaning similar to f_m , so that both can be used to characterize the pressure fluctuations in the frequency case, Eq. 33 can be used to explain the trend of \bar{f}_d against H_s/D_t qualitatively. However, we need to study the quantitative description of the relation between \bar{f}_d and H_s/D_t further. In Figure 9, the separation of the three curves corresponding to different tap heights can also be understood with Eq. 32.

Extensive experimentation indicates that the main trend of the major frequency of the power-spectral density and \bar{f}_d are similar, though the former is generally less than the latter. But the stability of the two parameters differs remarkably. We made a reproducibility comparison between the major frequency and the LPWA. Ten experimental runs were conducted under identical operating conditions. The results are listed in Table 3, along with their mean, standard deviation, and relative standard deviation. Evidently, the LPWA is statistically much more reproducible than the major frequency, which we feel is mainly due to the nonstationary feature of the pressure fluctuation. Using the major frequency implicitly

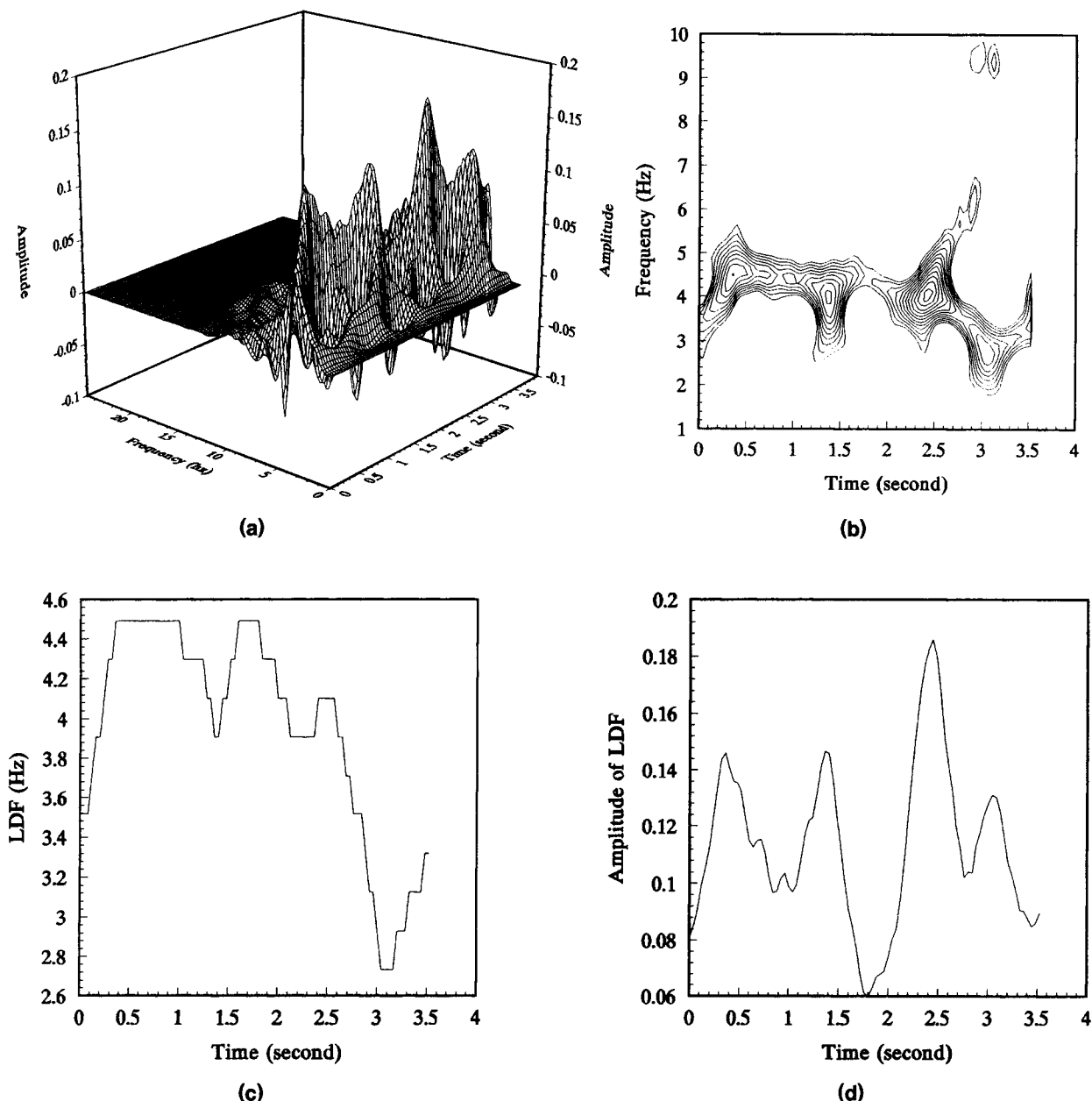


Figure 7. (a) WD of the signal in Figure 6(a); (b) contour of WD; (c) LDF of WD; (d) amplitude of LDF.

provokes the competition among the LDFs belonging to different times, which eventually causes instability. The LPWA avoids such conflict because it accounts for the LDFs jointly. Thus we think that the LPWA can reflect more faithfully and accurately the nature of the pressure fluctuation and the effect of bubbles than the major frequency. It can be regarded as a significant index for characterizing the quality of fluidization. Also, it may be useful in fault diagnosis in fluidized beds.

Conclusions

WD analysis has been used to analyze random pressure fluctuations from a gas-solid fluidized bed. The strong nonstationarity of the pressure fluctuations has been demon-

strated, thus showing how nonstationary methods can be used to analyze pressure fluctuations in fluidized beds. Our research also seems to indicate that the model proposed by Neogi et al. (1988) may not be the most appropriate one to demonstrate the nature of the pressure fluctuation signals in gas-solid fluidized beds. The form of the WD suggests that the signal may consist of successive impulses located around different time and frequency centers, and that most of the time only one local dominant frequency exists. A useful parameter of the LPWA, which can be considered as a natural generalization of the major frequency of power-spectral density in the nonstationary case, has been defined and successfully used to determine the local frequency information expressed in the WD of pressure-fluctuation signals. We made a preliminary study of the change in the LPWA under differ-

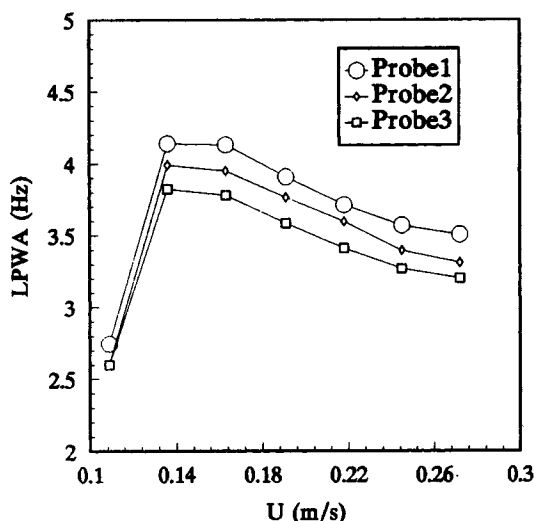


Figure 8. LPWA (f_d) vs. superficial gas velocity u and probe height, $H_s/D_t = 1.8$.

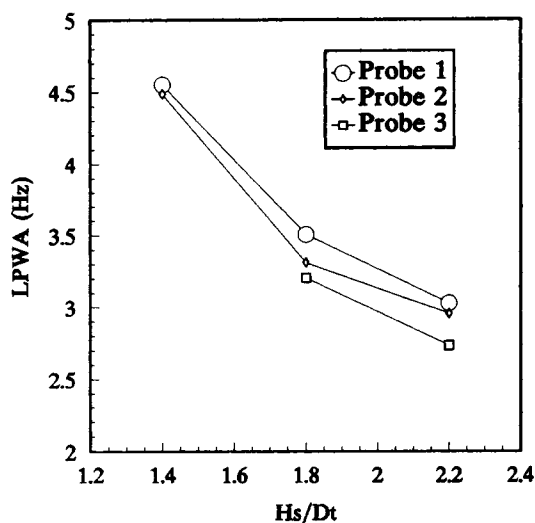


Figure 9. LPWA (f_d) vs. H_s/D_t , $u = 0.218$ m/s.

Table 3. A Comparison of the Statistical Reproducibility Between Major Frequency and LPWA*

Exp. No.	Major Frequency (Hz)	LPWA (Hz)
1	3.125	3.405
2	2.734	3.560
3	3.516	3.489
4	2.930	3.578
5	2.734	3.391
6	3.320	3.624
7	2.930	3.587
8	2.539	3.408
9	3.125	3.559
10	2.734	3.452

Statistics

Mean of major frequency = 2.969 (Hz)
 Standard deviation of major frequency = 0.304 (Hz)
 Relative standard deviation of major frequency = 10.2%
 Mean of LPWA = 3.505 (Hz)
 Standard deviation of LPWA = 0.087 (Hz)
 Relative standard deviation of LPWA = 2.5%

ent operating conditions, and the results show that it can well link with the change in the bubble phase, which is the major cause of the pressure fluctuation. This linkage promises to be a useful index for showing the quality of the fluidization. A comparison of the LPWA with the major frequency of the signal indicates that the LPWA is much more statistically reproducible, and we think the nonstationary feature is probably responsible for this result.

Acknowledgment

The research was supported by SINOPEC. We are deeply indebted to Professor Gantang Chen and the anonymous reviewers whose discerning comments improved the readability of the article.

Literature Cited

- Adamopoulos, P. G., J. K. Hammond, and J. S. Lee, "The Wigner Distribution, Multi-Equilibria Nonlinear Systems and Chaotic Behavior," *Proc. IEEE ICASSP*, 2216 (1988).
- Bailie, R. C., L. T. Fan, and J. J. Stewart, "Uniformity and Stability of Fluidized Beds," *AIChE J.*, **14**, 427 (1968).
- Bakshi, B. R., H. Zhong, P. Jinag, and L. S. Fan, "Analysis of Flow in Gas-Liquid Bubble Columns Using Multi-Resolution Methods," *Trans. Ind. Chem. Eng.*, **73**, 608 (1995).
- Boashash, B., "Wigner Analysis of Time Varying Signals and Application to Seismic Prospecting," *EUSIPCO 83*, North-Holland, Amsterdam, p. 703 (1983).
- Boashash, B., "Estimating and Interpreting the Instantaneous Frequency of a Signal, Part I, Part II," *Proc. IEEE*, **80**, 519 (1992).
- Carsky, M., M. Hartman, B. K. Ilyenko, and K. E. Makhern, "The Bubble Frequency in a Fluidized Bed at Elevated Pressure," *Powder Technol.*, **61**, 251 (1990).
- Chester, P., F. Taylor, and M. Doyle, "The Wigner Distribution in Speech Processing," *J. Franklin Inst.*, **318**, 415 (1984).
- Claasen, T. A. C. M., and W. F. G. Mecklenbrauker, "The Wigner Distribution—A Tool for Time-Frequency Signal Analysis, Part I, Part II, Part III," *Philips J. Res.*, **35**, 217, 276, 372 (1980).
- Cohen, L., "Time-Frequency Distribution—A Review," *Proc. IEEE*, **77**(7), 941 (1989).
- Darton, R. C., R. D. Lanauze, J. F. Davidson, and D. Harrison, "Bubble Growth Due to Coalescence in Fluidized Beds," *Trans. Ind. Chem. Eng.*, **55**, 274 (1977).
- Fan, L. T., T. H. S. Hiraoka, and W. P. Walawender, "Pressure Fluctuations in a Fluidized Bed," *AIChE J.*, **27**, 388 (1981).
- Fan, L. T., D. Neogi, M. Yashima, and R. Nassar, "Stochastic Analysis of a Three-Phase Fluidized Bed: Fractal Approach," *AIChE J.*, **36**, 1529 (1990).
- Fan, L. T., Y. Kang, D. Neogi, and M. Yashima, "Fractal Analysis of Fluidized Particle Behavior in Liquid-Solid Fluidized Beds," *AIChE J.*, **39**, 513 (1993).
- Flandrin, P., "Some Features of Time-Frequency Representation of Multicomponent Signals," *Proc. IEEE ICASSP*, **41B**(4), 1 (1984).
- Garudadri, H., M. P. Beddoes, A. P. Benguerel, and J. H. V. Gilbert, "On Computing the Smoothed Wigner Distribution," *Proc. IEEE ICASSP*, 1521 (1987).
- Harris, J. F., "On the Use of Window for Harmonic Analysis with the Discrete Fourier Transform," *Proc. IEEE*, **66**(1), 51 (1978).
- Huang, Y. W., L. T. Fan, J. C. Song, and N. Yutanl, "Pressure Fluctuations in a Gas-Solid Fluidized Bed with a Screen," *Ind. Eng. Chem. Process Des. Dev.*, **25**, 284 (1986).
- Imberger, J., and B. Boashash, "Application of the Wigner-Ville Distribution to Temperature Gradient Microstructure: a New Technique to Study Small Scale Variations," *J. Phys. Ocean.*, **16**, 1997 (1986).
- Kage, H., N. Iaskaki, H. Yamaguchi, and Y. Matsuno, "Frequency Analysis of Pressure Fluctuation in Fluidized Bed Plenum," *J. Chem. Eng. Jpn.*, **24**, 76 (1991).
- Kang, K. W., J. P. Sutherland, and G. L. Osberg, "Pressure Fluctuations in a Fluidized Bed with and without Screen Cylindrical Packings," *Ind. Eng. Chem. Fundam.*, **6**, 449 (1967).
- Kwon, H. W., K. Kang, S. D. Kim, M. Yashima, and L. T. Fan,

*All experiments were done under the following conditions: $u = 0.272$ m/s; $H_s/D_t = 1.8$; $h = 0.05$ m.

- "Bubble-Chord Length and Pressure Fluctuations in Three-Phase Fluidized Beds," *Ind. Eng. Chem. Res.*, **33**, 1852 (1994).
- Lee, G. S., and S. D. Kim, "Pressure Fluctuations in Turbulent Fluidized Beds," *J. Chem. Eng. Jpn.*, **21**, 515 (1988).
- Lirag, R. C., and H. Littman, "Statistical Study of the Pressure Fluctuations in a Fluidized Bed," *AIChE Symp. Ser.*, **67**(116), 11 (1971).
- Loeve, M., *Probability Theory*, Vol. II, Springer-Verlag, New York (1978).
- Martin, W., and P. Flandrin, "Analysis of Nonstationary Processes: Short Time Periodograms Versus a Pseudo Wigner Estimator," *EURASIP*, 455 (1983).
- Martin, W., and P. Flandrin, "Wigner-Ville Spectral Analysis of Nonstationary Processes," *IEEE Trans. Acoust. Speech, Signal Process.*, **ASSP-34**(4), 858 (1986).
- Moritomi, H., S. Mori, K. Araki, and A. Moriyama, "Periodic Pressure Fluctuations in a Gaseous Fluidized Bed," *Kagaku Kogaku Ronbunshu*, **6**, 392 (1980).
- Neogi, D., L. T. Fan, N. Yutani, R. Nassar, and W. P. Walawender, "Effect of Superficial Velocity on Pressure Fluctuations in a Gas-Solid Fluidized Bed: A Stochastic Analysis," *Appl. Stochastic Models Data Anal.*, **4**, 13 (1988).
- Priestley, M. B., "Evolutionary Spectra and Non-stationary Process," *J. Roy. Statist. Soc., Serial B*, **27**(2), 204 (1965).
- Shuster, W., and P. Kisliak, "The Measurement of Fluidization Quality," *Chem. Eng. Prog.*, **48**, 455 (1952).
- Stankovic, L., and S. Stankovic, "Wigner Distribution of Noisy Signals," *IEEE Trans. Signal Process.*, **SP-41**(2), 956 (1993).
- Verloop, J., and P. M. Heertjes, "Period Pressure Fluctuations in Fluidized Beds," *Chem. Eng. Sci.*, **29**, 1035 (1974).
- Ville, J., "Theorie et Applications de la Notion de Signal Analytique," *Cables Transm.*, **2**^A(1), 61 (1948).
- Welch, P. D., "The Use of Fast Fourier Transform of Estimation of Power Spectra: A Method Based on Time Averaging over Short, Modified Periodograms," *IEEE Trans. Audio Electroacoust.*, **AU-15**, 70 (1967).
- Wigner, E., "On the Quantum Correction for Thermodynamic Equilibrium," *Phys. Rev.*, **40**, 246 (1932).
- Winter, O., "Density and Pressure Fluctuations in Gas Fluidized Beds," *AIChE J.*, **14**, 427 (1968).

Manuscript received Mar. 4, 1996, and revision received Aug. 19, 1996.